A Combined ab Initio MO−MM Study on Isotacticity Control in Propylene Polymerization with Silylene-Bridged Group 4 Metallocenes. C_2 Symmetrical and Asymmetrical Catalysts

Tohru Yoshida,[†,‡,§] Nobuaki Koga,[†,§] and Keiji Morokuma*,[†,||]

Institute for Molecular Science, Okazaki 444, Japan, Polymer Synthesis, Yokkaichi Research Laboratory, Tosoh Corporation, 1-8, Kasumi, Yokkaichi 510, Japan, School of Informatics and Sciences, Nagoya University, Nagoya 464-01, Japan, and Cherry L. Emerson Center for Scientific Computation and Department of Chemistry, Emory University, Atlanta, Georgia 30322

Received May 30, 1995[⊗]

The isotactic control capabilities in propylene polymerization of various substituted *ansa*-metallocenes are evaluated with a combined ab initio MO−MM method. Steric energy controlling the isotacticity at the transition state is divided into the direct term (steric energy due to the catalyst−olefin interaction) and the indirect term (steric energy due to the catalyst−polymer and polymer−olefin interaction). Among group 4 bis(indenyl) and bis(tetrahydroindenyl) complexes, titanium complexes in general have a substantially better capability of producing an isotactic sequence over zirconium and hafnium analogs, due to the small atomic size of the central metal. To attain good stereoregulation, the substituents at the 2- and 4-positions of the indenyl-based metallocene are very important. However, analysis among congested indenyl-based catalysts suggests that, though the crowded transition structures in general provide better stereocontrol, overcrowding could reduce flexibility and lower stereoregulatory discrimination. An asymmetric catalyst allowing completely one-blocked insertion shows a high isotactic control. The present method reveals qualitatively the control factors of stereoregulation that are consistent with the experiment and may be used for prediction for unknown catalysts.

I. Introduction

Isotactic polypropylene is used in a wide field of applications for both commodity and technical uses, and its consumption is still growing rapidly.[1] Stereoregularity control in α-olefin polymerization is one of the most important capabilities of Ziegler−Natta-type catalysts.[1] The assumption that only heterogeneous catalysts efficiently produced isotactic polypropylene was challenged when Kaminsky and his co-workers discovered that homogeneous isotactic propylene polymerization could be achieved with stereorigid zirconocene catalysts, $CH_2CH_2(indenyl)_2ZrCl_2$, with substituents on the indenyl ligands, where the indenyl group generates a chiral field.[2] Since then, much attention has been paid to the ligand effects on stereoregulation for isotacticity and syndiotacticity in homogeneous propylene polymerization.[3] Substantial key advances have been made by Erker ($(RCp)_2MX_2$, Cp = cyclopentadienyl, R = alkyl or silylalkyl),[4a] Yamazaki ($Me_2Si(R'_2Cp)_2MX_2$, R′ = alkyl),[4b] Spaleck ($Me_2Si(R''$-indenyl$)_2MX_2$, R″ = alkyl and/or aryl),[4c−e] for isotactic stereoregulation, and Ewen ($Me_2C(Cp)$(fluorenyl)MX_2)[4f] for syndiotactic regulation.

Direct and indirect evidence supports the idea that the active species in the metallocene-based catalyst system is a d^0 alkyl complex.[5] Olefin monomers react alternately at the two vacant sites of the naked alkyl complex. When the direction of propylene insertion can be regulated by the C_2 symmetrical catalyst, each sequential insertion maintains the same stereochemistry resulting in the isotactic sequence, and with the C_s symmetrical catalyst, the insertion alternately takes place enantiomerically giving rise to a syndiotactic sequence, as shown schematically in Scheme 1A and B, respectively.[6]

† Institute for Molecular Science.
‡ Tosoh Corp.
§ Nagoya University.
|| Emory University.
⊗ Abstract published in *Advance ACS Abstracts,* December 15, 1995.

(1) (a) Quirk, R. P. *Transition Metal Catalyzed Polymerizations*; Cambridge University Press: Cambridge, U.K., 1988. (b) McAlpin, J. J. Worldwide Metallocene Conference, MetCon '94, Houston, TX, 1994. (c) Aulbach, M.; Küber, F; Spaleck, W. International Congress on Metallocene Polymers, Metallocenes '95, Brussels, Belgium, 1995. (d) Fink, G, Mülhaupt, R., Brintzinger, H. H., Eds. *Ziegler Catalysts*; Springer-Verlag: Berlin, 1995.

(2) Kaminsky, W.; Kulper, K.; Brintzinger, H. H; Wild, F. R. W. P. *Angew. Chem., Int. Ed. Engl.* **1985**, *24*, 507.

(3) (a) Keii, T., Soga, K., Eds. *Catalytic Polymerization of Olefin*; Elsevier: Amsterdam, 1986. (b) Kaminsky, W., Sinn, H., Eds. *Transition Metals and Organometallics as Catalysts for Olefin Polymerization*; Springer: New York, 1988.

(4) (a) Erker, G.; Nolte, R.; Tsay, Y.-H.; Krueger, C. *Angew. Chem., Int. Ed. Engl.* **1985**, *28*, 628. (b) Mise, T.; Miya, S.; Yamazaki, H. *Chem. Lett.* **1989**, 1853. (c) Spaleck, W.; Antberg, M.; Rohrmann, J.; Winter, A.; Bachmann, B.; Kiprof, P.; Behm, J.; Herrmann, W. *A. Angew. Chem., Int. Ed. Engel.* **1992**, *31*, 1347. (d) Spaleck, W.; Küber, F.; Winter, A.; Rohrman, J.; Bachmann, B.; Antberg, M.; Dolle, V.; Paulus, E. F. *Organometallics* **1994**, *13*, 954. (e) Spaleck, W.; Antberg, M.; Aulbach, M.; Bachmann, B.; Dolle, V.; Haftka, S.; Küber, F.; Rohrmann, J.; Winter, A. In *Ziegler Catalysts*; Fink, G., Mülhaupt, R., Brintzinger; H. H., Eds.; Springer-Verlag: Berlin, 1995; p 83. (f) Ewen, J. A.; Jones, R. I.; Razavi, A. *J. Am. Chem. Soc.* **1988**, *110*, 6255.

(5) (a) Breslow, D. S.; Newberg, N. R. *J. Am. Chem. Soc.* **1959**, *81*, 628. (b) Long, W. P.; Breslow, D. S. *J. Am. Chem. Soc.* **1960**, *82*, 1953. (c) Dyachkovskii, F. S.; Shilova, A. K.; Shilov, A. V. *J. Polym. Sci., Part C* **1967**, *16*, 2333. (d) Watson, P. L.; Roe, D. C. *J. Am. Chem. Soc.* **1982**, *107*, 6471. (e) Eisch, J. J.; Piotrowski, A. M.; Brownstein, Gabe, E. J.; Lee, F. L. *J. Am. Chem. Soc.* **1985**, *10*, 7219. (f) Alelyunas, Y. W.; Jordan, R. F.; Echols, S. F.; Borkowsky, S. L.; Bradley, P. K. *J. Am. Chem. Soc.* **1991**, *107*, 8091.

0276-7333/96/2315-0766$12.00/0

Scheme 1

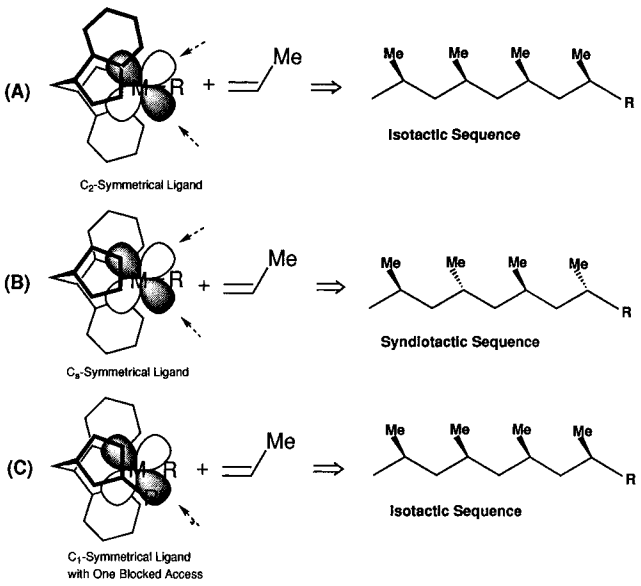

Two types of controlling mechanisms for stereoregulation have been proposed:[7] *direct* control by the chirality of the catalyst, sometimes called catalyst control or enantiomorphic site control, and *indirect* control by the conformation of the last inserted monomer unit, also called chain-end control. Corradini et al., on the basis of conformation analysis by calculation of nonbonded interaction energies, suggested that the stereoregulation is indirectly controlled.[8] Rappé reported molecular mechanics (MM) results that support direct control due to the chirality of the catalysts.[9] In these studies, the "activated complex" at which the energy was evaluated looks more like an olefin π-complex rather than a four-centered transition state (TS).

Since the selectivity is actually determined at the TS, a reasonable structure of the TS is required to obtain a reliable conclusion.[10] In our previous theoretical study, we determined, with an ab initio molecular orbital (MO) method, the structures of the reactant, the ethylene π-complex, TS, and the product for ethylene insertion into the Zr−C bond of $(H_2SiCp_2)ZrMe^+$ following the widely accepted Cossee mechanism[11] and studied with MM calculations the origin of regio- and stereoselectivity in propylene polymerization by introducing alkyl substituents to the ab initio-determined structures of the TS and the π-complex for ethylene insertion. As a result we showed that the direct influence of alkyl substituents on Cp rings is small and the selectivitiy is determined *indirectly* via the steric interaction between the polymer chain and the olefin.[10]

Subsequently, we reported the extension of the ab initio MO study[12a] in which we compared the catalytic activities among group 4 (Ti, Zr, Hf) silylene-bridged metallocene cations in the ethylene insertion reaction, by restricted quadratic configuration interaction with single and double excitations (RQCISD)[13] based on the restricted Hartree−Fock (RHF)[14] optimized structures. The propagation step includes at least two transition states: the first TS is for the olefin insertion reaction and is located midway between the π-complex and the γ-agostic product (direct product), and the second TS is for isomerization of the product and comes between the γ-agostic and the β-agostic product. Some important features reflecting the size of the central metal became clear and are consistent with the experimental results; the activation energies for all the three metals are low, the order of the activity decreases in the order Zr ≥ Hf > Ti,[15] and Hf among the three metals should give the longest polymer chain with narrowest polydispersity. Some recent theoretical studies gave no or a very small barrier for insertion.[12b−e] However, these findings have been attributed to the fault of the theoretical methods used in such calculations.[12a]

The goal of the present paper is mainly to study the mechanism of isotactic stereoregulation at the insertion TS by the substituent effect of *ansa*-group 4 metallocenes with C_2 symmetrical ligands, providing a qualitative measure for explanation of the control factors in the stereoregulation in propylene polymerization. For evaluation of the stereoregulatory ability, full ab initio MO calculation would provide more quantitative results but is too computer time consuming. Therefore, we used the same approach as we did before, i.e., a combination of ab initio MO and MM methods. Here we will present the results for C_2 symmetrical $H_2Si(indenyl)_2MMe^+$ **1** and $H_2Si(tetrahydroindenyl)_2MMe^+$ **2** (M = Ti, Zr,[4c−e] and Hf[4c]) and, for an asymmetrical H_2Si(3-*tert*-butylCp)(fluorenyl)$ZrMe^+$ Zr**3a**.[16] Especially for bis(indenyl)zirconium catalysts Zr**1a**−Zr**1k**,[4c−e] various substituents will be examined to rationalize their steric effects. After an explanation of computational method in section II, we will discuss in section III-1 RHF-optimized structures for reference catalysts, transition states of which will used for the MM calculations. In section III-2, various substituted *ansa*-metallocenes will be examined with the MM calculation. In section IV, we compared the calculation with the corresponding experimental results. Concluding remarks will be given in section V.

II. Method of Calculation

The geometry optimizations of the reactants and the TS's in the ethylene insertion for H_2Si(Cp)(fluorenyl)-

(6) Ewen, J. A.; Elder, M. J.; Jones, R. L.; Haspeslagh, L.; Atwood, J. L.; Bott, S. G. *Makromol. Chem., Makromol. Symp.* **1991**, *48/49*, 253.

(7) Ledwith, A.; Sherington, D. C. *Reactivity, Mechanism, and Structure in Polymer Chemistry*; Wiley-Interscience: New York, 1974.

(8) (a) Cavallo, L.; Guerra, G.; Vacatello, M.; Corradini, P. *Macromolecules* **1991**, *24*, 1784. (b) Corradini, P.; Guerra, G.; Cavallo, L.; Moscardi, G.; Vacatello, M. In *Ziegler Catalysts*; Fink, G., Mülhaupt, R., Brintzinger, H. H., Eds.; Springer-Verlag: Berlin, 1995; p 237.

(9) (a) Rappé, A. K.; Castonguay, L. A. *J. Am. Chem. Soc.* **1992**, *114*, 5832. (b) Hart, J. R.; Rappé, A. K. *J. Am. Chem. Soc.* **1993**, *115*, 6159.

(10) (a) Kawamura-Kuribayashi, H.; Koga, N.; Morokuma, K. *J. Am. Chem. Soc.* **1992**, *114*, 8687. (b) Koga, N.; Yoshida, T.; Morokuma, K. Symposium on 40 Years of Ziegler Catalysts, Freiburg, Germany, 1993. (c) Koga, N.; Yoshida, T.; Morokuma, K. In *Ziegler Catalysts*; Fink, G., Mülhaupt, R., Brintzinger, H. H., Eds.; Springer-Verlag: Berlin, 1995; p 275.

(11) Cossee, P. *J. Catal.* **1964**, *3*, 80.

(12) (a) Comparison has also been made with recent theoretical studies[12b−e] which gave no or a quite small barrier: Yoshida, T.; Koga, N.; Morokuma, K. *Organometallics* **1995**, *14*, 746. (b) Weiss, H.; Haase, F.; Ahlrichs, R. *J. Am. Chem. Soc.* **1994**, *116*, 4919. (c) Woo, T. K.; Fan, L.; Ziegler, T. *Organometallics* **1994**, *13*, 432. (d) Woo, T. K.; Fan, L.; Ziegler, T. *Organometallics* **1994**, *13*, 2252. (e) Meier, R. J.; Doremaele, G. H. J. v.; Iarlori, S.; Buda, F. *J. Am. Chem. Soc.* **1994**, *116*, 7274.

(13) Raghavachari, K.; Pople, J. A. *Int. J. Quant. Chem.* **1981**, *20*, 167.

(14) Roothaan, C. C. J. *Rev. Mod. Phys.* **1951**, *23*, 69.

(15) Bochmann, M.; Lancaster, S. J. *J. Organomet. Chem.* **1992**, *434*, C1.

(16) (a) Ewen, J. A. Symposium on 40 Years of Ziegler Catalysts, Freiburg, Germany, 1993. (b) Ewen, J. A.; Elder, M. J. In *Ziegler Catalysts*; Fink, G., Mülhaupt, R., Brintzinger, H. H., Eds.; Springer-Verlag: Berlin, 1995; p 99.

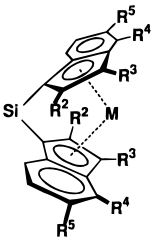

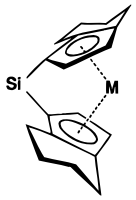

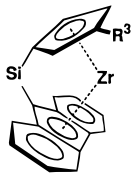

	R^2	R^3	R^4	R^5
1: M=Ti,Zr,Hf	H	H	H	H
Zr1a	Me	H	H	H
Zr1b	H	Me	H	H
Zr1c	Me	H	Me	H
Zr1d	Me	H	Et	H
Zr1e	Me	H	^{iso}Pro	H
Zr1f	H	H	^{iso}Pro	H
Zr1g	Me	H	^{tert}Bu	H
Zr1h	Me	H	Ph	H
Zr1i	Me	H	3-Tol	H
Zr1j	Me	H	1-Nap	H
Zr1k	Me	H	4,5-Benz	

2: M=Ti, Zr, Hf

Zr3: R^3=H
Zr3a: R^3=^{tert}Bu

Chart 1

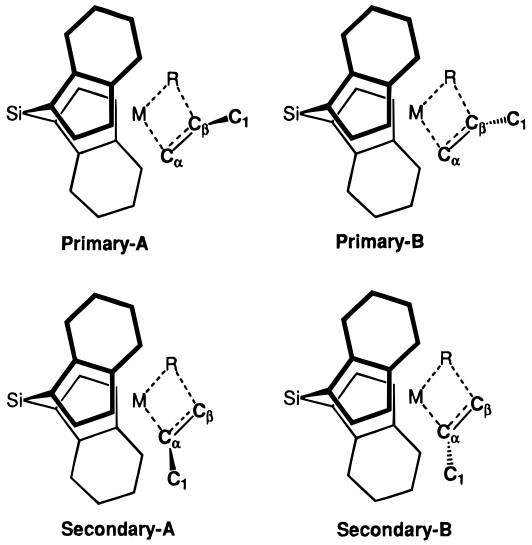

$ZrMe^+$ (Zr**3**) and $H_2SiCp_2MMe^+$ (M = Ti, Zr, Hf) **4** were carried out with the ab initio RHF energy gradient method.[17] For group 4 metals, the split-valence basis functions (Ti, 311/311/41 for 3s4s/3p4p/3d; Zr, 311/311/31 for 4s5s/4p5p/4d; Hf, 311/311/21 for 5s6s/5p6p/5d) were used with the Hay and Wadt effective core potentials.[18] For atoms of the silylene-bridged ligand that is a spectator and does not participate directly in the present reaction, we used the minimal STO-3G[19a] basis functions, and for CH_3 and C_2H_4 the split-valence 3-21G[19b] basis functions. The equilibrium structure **4** was optimized under C_s symmetry and the transition state **4**TS (from now on to denote a transition state, we add "TS" after the number for the corresponding catalyst) under C_1 symmetry, where the $H_2SiCp_2M^+$ fragment was assumed to maintain local C_s symmetry and the Cp moiety a local C_{5v} symmetry. For Zr**3** and Zr**3**TS, the basis sets used were the same as above, and the optimization was carried out under C_1 symmetry with locally maintaining C_{2v} symmetry both for Cp and the fluorenyl moiety.

In MM calculation, some of the hydrogen atoms in the ab initio-optimized geometries were replaced by substituents and the Cartesian coordinates of only these newly considered substituents were optimized, while the ab initio-optimized geometries (excluding the replaced hydrogen atoms) were frozen. For example, in the insertion of propylene to the indenyl catalyst **1**, the Cartesian coordinates of the methyl group of propylene, the butadienylene fragment of indenyl, the substituents on the indenyl, and the growing polymer chain were optimized. We used the MM2 force field and program.[20]

The sp^3 carbon parameters were adopted for alkyl carbons and the sp^2 carbon parameters for ethylene carbons. The central metal was treated as a dummy atom having zero force constants. For all other atoms, the standard parameters were used.

In the insertion of propylene, there are four possible transition state structures, two modes for primary insertion and other two for secondary insertion, as illustrated in Chart 1. In order to evaluate stereoregulatory capability, one has to compare the differences in the activation barrier among these four possible TS's. Since the electronic energy for the ab initio-optimized model (unsubstituted) TS is common, we will compare the steric energies for the four TS's at their most stable conformation for the substituents and the polymer chain.

III. Results and Discussion

1. RHF-Optimized Structures of Reactant and TS in Ethylene Insertion. At first we will briefly discuss the already published[10] RHF-optimized geometries for the reactant and the ethylene insertion transition state for $H_2Si(Cp)_2MMe^+$, **4** and **4**TS, and compare these with the new results for H_2Si(fluorenyl)-(Cp)$ZrMe^+$, Zr**3** and Zr**3**TS, as shown in Figure 1. All these structures will be used as the starting points for the MM optimization of substituted systems.

The structures of the reactants $H_2Si(Cp)_2MMe^+$ **4** are consistent with the experimental results.[10] Relaxation of local symmetry constraints mentioned in the method section for Zr**4** changed the geometry very little, indicating that such constraints are reasonable. **4**TS's have nearly coplanar $MC_\alpha C_\beta C_\gamma$ four-membered reaction centers and show signs of agostic interaction between M and C_γ–H, a short M–C_γ, and a long C_γ–H distance. Reflecting the atomic radii of three metals, Ti**4**TS is the most compact, with Zr**4**TS and Hf**4**TS substantially looser. Though not shown in Figure 1, changes in the C_{Cp}–Si–C_{Cp} and $Cp_{centroid}$–M–$Cp_{centroid}$ angles from the reactants to the TS's are small, reflecting the rigid nature of the H_2Si bridge.

(17) All the calculations were carried out with the following programs: GAUSSIAN 90 (Frisch, M. J.; Head-Gordon, M.; Trucks, G. W.; Foresman, J. B.; Schlegel, H. B.; Raghavachari, K.; Robb, M. A.; Binkley, J. S.; Gonzales, C.; DeFrees, J. S.; Fox, J. S.; Whiteside, R. A.; Seeger, R.; Melius, C. F. ; Baker, J.; Martin, R. L.; Kahn, L. R.; Stewart, J. J. P.; Topiol, S.; Pople, J. A. Gaussian, Inc., Pittsburgh, PA, 1990) and GAUSSIAN 92 (Frisch, M. J.; Trucks, G. W.; Head-Gordon, M.; Gill, P. M. W.; Wong, M. W.; Foresman, J. B.; Johnson, B. G.; Schlegel, H. B.; Robb, M. A.; Replogle, E. S.; Gomperts, R.; Andres, J. L.; Raghavachari, K.; Binkley, J. S.; Gonzalez, C.; Martin, R. L.; Fox, D. J.; Defrees, D. J.; Baker, J.; Stewart, J. J. P.; Pople, J. A. Gaussian, Inc., Pittsburgh PA, 1992).

(18) Hay, P. J.; Wadt, W. R. *J. Chem. Phys.* **1985**, *82*, 299.

(19) (a) Collins, J. B.; Schleyer, P. v. R.; Binkey, J. S.; Pople, J. A. *J. Am. Chem. Soc.* **1976**, *64*, 5142. (b) Gordon, M. S.; Binkley, J. S.; Pople, J. A. *J. Am. Chem. Soc.* **1982**, *104*, 2797.

(20) (a) Allinger, N. L.; Yuh, Y. *QCPE* **1980**, *No. 12*, 395. (b) Burkert, U.; Allinger, N. L. *Molecular Mechanics*; American Chemical Society: Washington, DC, 1982.

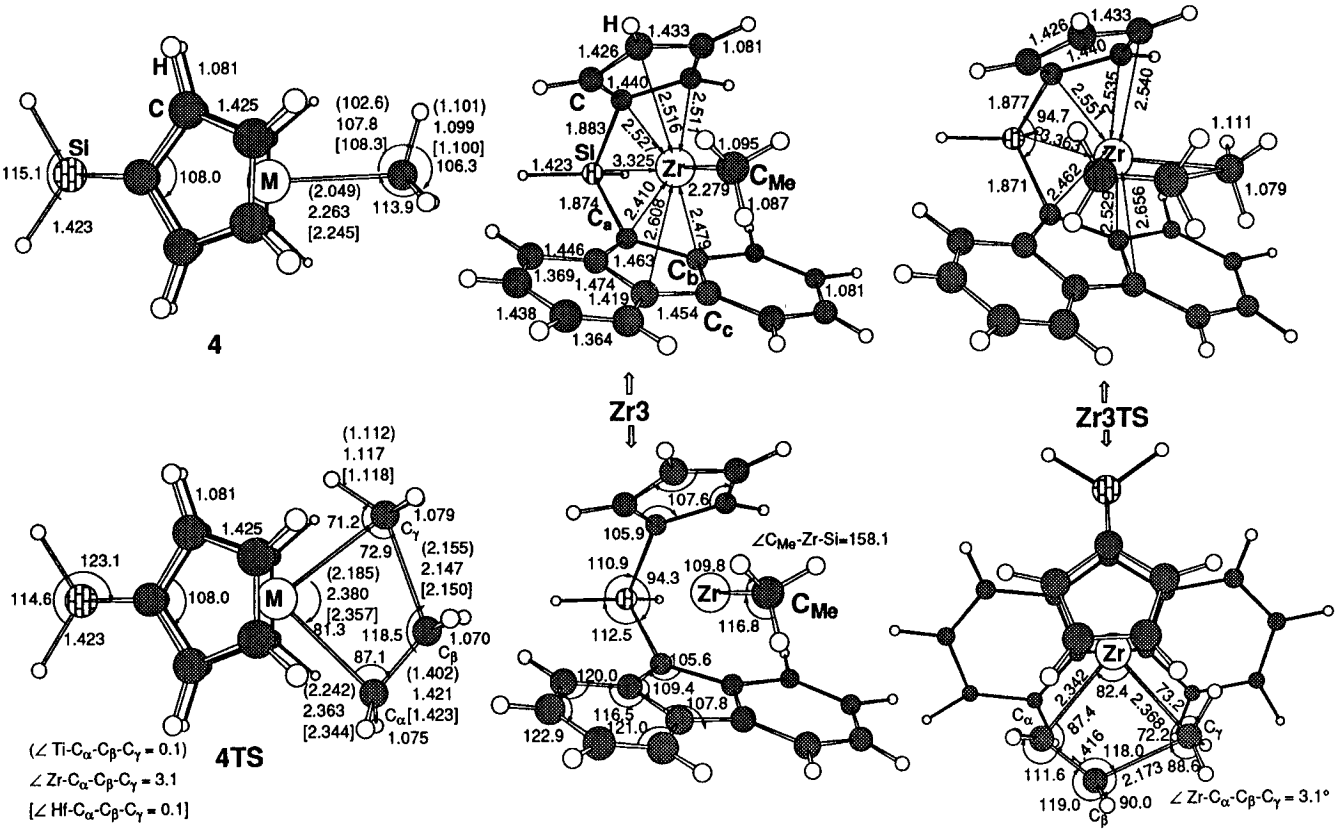

Figure 1. RHF-optimized structures of $H_2SiCp_2MMe^+$ **4** and $H_2Si(3\text{-}^t\text{BuCp})$(fluorenyl)$ZrMe^+$ (Zr**3**) and their TS's for ethylene insertion, **4**TS and Zr**3**TS. For **4** and **4**TS, the numbers in parentheses are for M = Ti, without parentheses for M = Zr, and in brackets for M = Hf.

In the reactant H_2Si(fluorenyl)(Cp)$ZrMe^+$ Zr**3**, all Zr−C_{Cp} distances are similar (2.527, 2.511, and 2.516 Å). However, two Zr−C distances (2.410 and 2.479 Å) of the Cp part in the fluorenyl group are shorter than the other Zr−C distance (2.608 Å), indicating that while the Cp ring coordinates in the η^5-mode, the fluorenyl coordination is in the η^3-mode. In the Cp part of the fluorenyl moiety, the π-orbital of the carbon (C_a) connected with silicon is bonded more strongly to the central metal than that of C_b and C_c, as judged from the zirconium and carbon distances.[21] Two benzene moieties of the fluorenyl have butadiene-like conjugated double bonds of 1.364 and 1.369 Å. Such a geometrical feature is in good agreement with the experimental results in Me_2C(Cp)-(fluorenyl)$HfCl_2$.[4e] One also notices that C_{Me}−Zr−Si atoms of Zr**3** are not collinear, with the angle of 158.1°.

Compared with Zr**4**TS, the C_{Cp}−Si−C_{Cp} angle for Zr**3**TS becomes wider only by 0.4°, and the C−Zr distances for both the Cp and the fluorenyl become longer by 0.05 Å. Between Zr**4**TS and Zr**3**TS, the twist angle of the four-membered reaction center, ∠Zr−C_α−C_β−C_γ = 3.1°, is unchanged. Geometrical features in Zr**3** are well conserved in the Zr**3**TS, as seen in Zr**4** and **4**TS. One of the C_{Me}−H bonds in Zr**3**TS is longer than the normal C−H bond[22] showing the agostic interaction, as seen in Zr**4**TS.[23] Such a rigidity, also seen in the cyclopentadienyl analogs **4**'s and **4**TS's, can be attributed to the bridged structure[24] and would make the tacticity control easier than in the nonbridged catalyst.[10]

2. Isotactic Stereoregulation in Propylene Polymerization with Group 4 C_2 Symmetrical Metallocenes. A. $H_2Si(indenyl)_2MR^+$ 1 and $H_2Si(tetrahydroindenyl)_2MR^+$ 2. For evaluation of regio- and stereoregulatory capabilities, we have to compare among the four possible TS's in Chart 1 the differences in the total energy, which in the present model are equal to the differences in the MM steric energy.

The MM optimization of the four transition states, primary-A, primary-B, secondary-A, and secondary-B of Chart 1, for propylene insertion into **1** and **2** has been carried out for the structures of substituents, based on the RHF-optimized structures of the model transition state **4**TS. The resultant steric energies, relative to primary-A for all the cases, are shown in Table 1. Our previous MM calculations for propylene insertion with $H_2Si(R_nCp)_2ZrMe^+$ have shown that the primary TS's are more stable than the secondary TS's.[10] Therefore, the energy difference between the primary-A TS and the primary-B TS should determine isotactic stereoregulation; if the difference is large, the propylene monomer will insert exclusively via only one TS providing isotactic sequence. The primary-A TS should be more favorable than the primary-B TS, because the Si−M−C_β is not collinear at the model TS (Figure 1) with ∠Si−M−C_β of 167.5° (Ti), 173.0° (Zr), and 174.1° (Hf) and the methyl group of inserting propylene in the primary-B TS should have closer contact with the indenyl moiety than that in the primary-A TS.

(21) Such geometrical feature was also detected in X-ray analysis of $(C_5Me_5)(PPh_3)Rh(C_2H_4)$: Zocchi, M; Porzio, W. *J. Am. Chem. Soc.* **1978**, *100*, 2048.

(22) With 3-21G optimization at the RHF level, the C_{Me}−H length of the propylene is 1.085 Å.

(23) Leclerc, M. K.; Brinzinger, H. H. *J. Am. Chem. Soc.* **1995**, *117*, 1651.

(24) Endo, J.; Koga, N.; Morokuma, K. *Organometallics* **1993**, *12*, 2777.

Table 1. Relative Steric Energies (in kcal/mol) at the Transition States for Propylene Insertion to Catalysts 1 and 2[a]

		primary insertion		secondary insertion	
catalyst	R[b]	primary-A	primary-B	secondary-A	secondary-B
Ti**1**	Me	0.0	3.8	13.3 (0.0)[c]	48.6 (35.3)
	$[CH_2CHMe]Me$	0.0	12.5	12.9 (0.0)	48.0 (35.1)
	$[CH_2CHMe]_2Me$	0.0	10.5	12.2 (0.0)	47.4 (35.2)
	$[CH_2CHMe]_3Me$	0.0	11.3	10.6 (0.0)	45.8 (35.2)
Zr**1**	Me	0.0	0.4	10.5 (0.0)	32.1 (21.6)
	$[CH_2CHMe]Me$	0.0	5.6	8.9 (0.0)	30.5 (21.6)
	$[CH_2CHMe]_2Me$	0.0	5.0	8.5 (0.0)	30.2 (21.7)
	$[CH_2CHMe]_3Me$	0.0	5.5	8.4 (0.0)	30.0 (21.6)
Hf**1**	Me	0.0	0.1	10.9 (0.0)	34.5 (23.6)
	$[CH_2CHMe]Me$	0.0	5.1	9.5 (0.0)	33.1 (23.6)
	$[CH_2CHMe]_2Me$	0.0	5.3	9.3 (0.0)	32.8 (23.5)
	$[CH_2CHMe]_3Me$	0.0	5.1	9.5 (0.0)	33.1 (23.6)
Ti**2**	Me	0.0	2.4	13.3 (0.0)	32.5 (19.2)
	$[CH_2CHMe]Me$	0.0	12.3	12.9 (0.0)	32.1 (19.2)
Zr**2**	Me	0.0	0.5	10.5 (0.0)	25.7 (15.2)
	$[CH_2CHMe]Me$	0.0	5.7	8.7 (0.0)	24.0 (15.3)
Hf**2**	Me	0.0	0.3	11.4 (0.0)	28.3 (16.9)
	$[CH_2CHMe]Me$	0.0	5.4	9.8 (0.0)	26.7 (16.9)

[a] Steric energies are shown relative to the primary-A mode. [b] R denotes the polymer chain, as shown in Chart 1. [c] Values in parentheses are the steric energies relative to the secondary-A mode.

In the initiation stage of polymerization, R in Chart 1 is the alkyl group of the original catalyst. When R = Me is used to represent this stage, the energy difference between the primary-A and -B is 3.8 kcal/mol for Ti**1** and the corresponding differences for Zr**1** and Hf**1** are 0.4 and 0.1 kcal/mol, respectively, as shown in Table 1. In the present calculation, we freeze the TS geometry of **4**TS at that of the model reaction, whereas in reality the TS structure will relax to reduce steric repulsion, and thus these energy differences should be considered as the upper limit. Therefore, one can conclude that in the initiation stage the energy difference is small and the stereoregulation is poor. One can also consider these energy differences as the result of a *direct* steric effect between the inserting olefin and the indenyl group, as the steric effect due to R is negligible, and conclude that the stereoregulation via direct ligand−olefin interaction for this catalyst is not significant.

After the first propylene has been inserted, the polymer chain R is isobutyl and at the next polymerization stage the energy differences between the two primary modes are 12.5 (Ti), 5.6 (Zr), and 5.1 (Hf) kcal/mol. One can see a remarkable gain in the energy difference from the initiation stage, by 8.7 (Ti), 5.2 (Zr), and 5.0 (Hf) kcal/mol. The energy difference is now large enough to ensure a very good stereoselectivity. Since the amount of the direct steric interaction between the inserting olefin and the indenyl group is considered unchanged from the initiation stage, the gain in steric energy difference can be attributed to the *indirect* steric energy, i.e., the steric energy due to the interaction between the inserting olefin and the polymer chain, whose conformation has been determined so as to minimize the steric repulsion from the indenyl group, as seen in the case of $H_2Si(CpMe_n)_2ZrR^+$ ($n = 0-2$).[10] The direct and indirect control energies thus determined for **1** and **2** are summarized in the upper half of Table 2. One notices that the indirect term is much more important in all the metals for **1** and **2**.

In subsequent insertion of the third and fourth olefin molecules, where the MM calculation was carried out by maintaining the isotactic sequence of the propagating polymer chain R, the changes in the relative energy are small, as seen in Table 1, indicating that the indirect steric energy is determined by the last inserted monomer and that the polymer chain end away from the reaction center does not participate in the stereoregulation. The ability of the catalyst for stereoregulation can be characterized by one monomer unit.

Table 2. Direct and Indirect Control Steric Energies (in kcal/mol) at the Transition State for Propylene Insertion for Varieties of Catalysts

	direct control	indirect control		direct control	indirect control
Ti**1**	3.8	8.7	Zr**1d**	2.1	5.8
Zr**1**	0.4	5.2	Zr**1e**	3.8	10.0
Hf**1**	0.1	5.0	Zr**1f**	4.0	5.1
Ti**2**	2.4	9.9	Zr**1g**	2.1	1.7
Zr**2**	0.5	5.2	Zr**1h**	2.0	14.7
Hf**2**	0.3	5.1	Zr**1i**	1.4	6.8
Zr**1a**	0.8	6.2	Zr**1j**	2.0	9.6
Zr**1b**	−1.1	3.9	Zr**1k**	2.0	6.1
Zr**1c**	2.5	6.3			

[a] Catalyst control. [b] Polymer chain-end control.

As seen in Table 1, among the three metals Ti gives the largest energy difference between the two primary transition states as well as between the best primary and the best secondary transition states, suggesting that the Ti catalyst should have the highest intrinsic ability of both regio- and stereoselectivities. Ti**1** and Ti**2**, having the most crowded TS due to the smallest atomic size among the group 4 metals, provide the largest steric repulsion and hence the largest discrimination, in both the direct and indirect steric interactions. Experimentally, the stereoregulatory capability or the fraction of the *mmmm* pentad in the polymer changes slightly: 91.6% (Ti), 94.6% (Zr), and 88.5% (Hf) for propylene polymerization using C_2 symmetrical $Me_2Si(MeCp)_2$-MMe^+ even at 20 °C.[25] We feel that the discrepancy between the above theoretical result and this experiment is due to the lower stability of the Ti complex in the experiment. In this experiment, Zr and Hf catalysts maintain the stereoregulatory ability up to 60 °C, with

(25) To the best of our knowledge, only one experimental result comparing the stereoregulatory capability among three metals has been reported: Yano, A.; Yamada, S.; Sone, M.; Akimoto, A. Third Workshop on Polymerization and Application between Japan and Korea, Seoul, Korea, 1991.

Table 3. Relative Steric Energies (in kcal/mol) at the Transition States for Propylene Insertion to Catalysts Zr1a to Zr1k[a]

		primary insertion		secondary insertion	
catalyst	R[b]	primary-A	primary-B	secondary-A	secondary-B
Zr**1**	Me	0.0	0.4	10.5 (0.0)[c]	32.1 (21.6)
	[CH_2CHMe]Me	0.0	5.6	8.9 (0.0)	30.5 (21.6)
Zr**1a**	Me	0.0	0.8	12.3 (0.0)	32.4 (21.0)
	[CH_2CHMe]Me	0.0	7.0	10.2 (0.0)	30.8 (20.6)
Zr**1b**	Me	0.0	−1.1	15.4 (0.0)	30.3 (14.9)
	[CH_2CHMe]Me	0.0	2.8	13.7 (0.0)	28.7 (15.0)
Zr**1c**	Me	0.0	2.5	9.9 (0.0)	30.7 (20.8)
	[CH_2CHMe]Me	0.0	8.8	8.4 (0.0)	28.8 (20.4)
Zr**1d**	Me	0.0	2.1	9.8 (0.0)	30.0 (20.2)
	[CH_2CHMe]Me	0.0	7.9	8.0 (0.0)	28.6 (20.6)
Zr**1e**	Me	0.0	3.8	16.9 (0.0)	40.3 (23.4)
	[CH_2CHMe]Me	0.0	13.8	12.3 (0.0)	35.8 (23.5)
Zr**1f**	Me	0.0	4.0	5.2 (0.0)	32.2 (27.0)
	[CH_2CHMe]Me	0.0	9.1	3.6 (0.0)	30.3 (26.7)
Zr**1g**	Me	0.0	2.1	4.6 (0.0)	24.5 (19.9)
	[CH_2CHMe]Me	0.0	3.8	2.1 (0.0)	22.5 (20.4)
Zr**1h**	Me	0.0	2.0	14.1 (0.0)	34.5 (20.4)
	[CH_2CHMe]Me	0.0	16.7	12.2 (0.0)	32.7 (20.5)
Zr**1i**	Me	0.0	1.4	11.7 (0.0)	36.5 (24.8)
	[CH_2CHMe]Me	0.0	8.2	10.0 (0.0)	34.9 (24.9)
Zr**1j**	Me	0.0	2.0	12.0 (0.0)	40.0 (28.0)
	[CH_2CHMe]Me	0.0	11.6	10.5 (0.0)	38.8 (28.3)
Zr**1k**	Me	0.0	2.0	10.4 (0.0)	33.6 (23.2)
	[CH_2CHMe]Me	0.0	8.1	6.7 (0.0)	29.7 (23.0)

[a] Steric energies are shown relative to the primary-A mode. [b] R denotes the polymer chain, as shown in Chart 1. [c] Values in parentheses are the steric energies relative to the secondary-A mode.

the melting point (T_m) of the resulting polymers at ~145 °C. However, the Ti catalyst abruptly decreases the stereoregulatory ability, as the polymerization temperature rises, i.e., T_m = 105 °C at 60 °C. The bond strengths increase in accord with increasing atomic number: Ti ≪ Zr < Hf.[26] Since the Ti catalyst with the weakest bond strength among the three metals will be affected most by temperature,[27] Ti could lose the catalyst structure at higher temperature resulting in lower stereoregulatory capability. What the present theoretical result suggests is that, if everything else is the same, a Ti catalyst should show the highest intrinsic stereoregulation among the three metal catalysts and the stereoregulatory order would be Ti ≫ Zr ≈ Hf, in accord with the atomic radii of the central metals.

From these results, we may conclude that the stereoregulation in propylene polymerization by the catalysts **1** is controlled indirectly by the ligand of the C_2 symmetric catalyst, as illustrated in Scheme 2, in agreement with our previous studies.[10] Before the monomer arrives, the propagating polymer chain finds a conformation minimum to avoid steric repulsion against the indenyl ligand of the catalyst. When the propylene monomer arrives, it is directed to the insertion in the primary-A mode by steric interaction with the propagating polymer chain. The selectivity is improved by the last inserted monomer unit, resulting in the formation of an isotactic sequence.

Now we turn our attention to regioselectivity. For every metal studied here the lower of the primary insertion TS's, primary-A, has a substantially (8 kcal/mol or more) smaller barrier height than the lower of the secondary insertion TS's, secondary-A. This is consistent with the experimental observation that primary insertion is dominant in propylene polymerization by metallocene catalysts.[28a−d] However, the dominant primary insertion may be controlled in part by an electronic preference in addition to the steric factor.[28e]

Scheme 2. Indirect Control of Stereoregularity: Determination of the Conformation of the Polymer Chain End

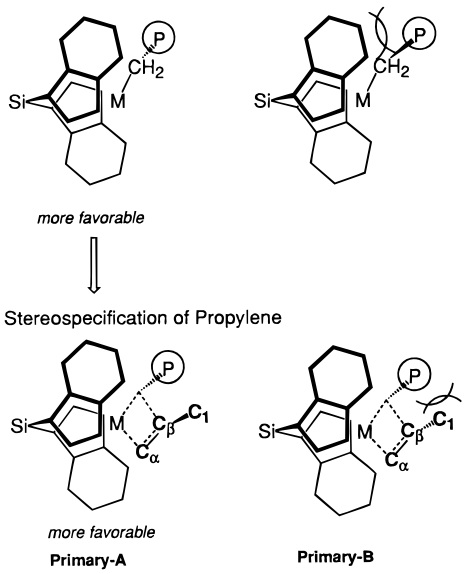

The energy difference between the secondary-A and the secondary-B is almost constant, suggesting that the indirect effect in the secondary insertion is negligible (see values in parentheses in Table 3). This would be understandable, considering the long distance between the polymer and the methyl group of the inserting propylene. Only the direct effect from the steric interaction between the ligand and the inserting propylene discriminates two secondary insertions.

In the primary modes, the propagating polymer chain has closer steric contact with the methyl group of the

(26) Cardin, D. J., Lappert, M. F., Raston, C. L., Eds. *Chemistry of Organo-Zirconium and -Hafnium Compounds*; John Wiley & Sons: New York, 1986; p 16.

(27) Ewen, J. A.; Haspeslagh, L.; Atwood, J. L.; Zhang, H. *J. Am. Chem. Soc.* **1987**, *109*, 6544.

inserting propylene than in the secondary modes and thus destabilizes the primary TS's. In other words, in the initiation stage the error in stereoregularity should occur mainly via participation of the primary-B mode, while in the propagation stage, especially for Ti**1**, the error may occur also via the secondary-A mode as well. This can be supported by the fact that the energy difference between the primary-B and the secondary-A becomes smaller as the polymer chain grows.

For the bis(tetrahydroindenyl) derivatives **2**, the direct control energies in the primary insertions are 2.4 (Ti), 0.3 (Zr), and 0.3 kcal/mol (Hf), and the indirect control energies are 9.9 (Ti), 5.2 (Zr), and 5.1 kcal/mol (Hf), as shown in Tables 1 and 2. Thus the bis(tetrahydroindenyl) catalyst **2** has an ability for stereoregulation comparable to that of the bis(indenyl) catalyst **1**.[2,4b,c,27] Here again one can recognize the size effect of the central metal; the tetrahydroindenyl catalyst Ti**2**, having the smallest atomic radius among the three central metals, has the largest control energy for high tacticity, as mentioned above.

B. Alkyl Substitution of $H_2Si(Indenyl)_2ZrMe^+$ Zr1a−Zr1g. Next, our attention is focused on the stereoregulation by the C_2-symmetrically alkyl-substituted $H_2Si(indenyl)_2ZrMe^+$, Zr**1a**−Zr**1g**. The relative steric energies at the olefin insertion transition states for various insertion modes are shown in Table 3, and the direct and indirect control steric energies, derived using the method[10] discussed above, are shown in the lower half of Table 2.

In Zr**1a**, where a methyl group is introduced at the 2-position of indenyl (R^2 = Me) in Zr**1**, stereoselection in primary insertion in the initiation stage is only slightly improved, with the direct control energy of 0.8 vs 0.4 kcal/mol for Zr**1**. However, in the propagation stage, the indirect control energy (6.2 kcal/mol for Zr**1a** vs 5.2 kcal/mol for Zr**1**) caused by the methyl−polymer chain interaction becomes effective, which should improve the stereoregularity. In Zr**1**, as seen in the MM2-optimized TS structures in the propagation stage (R = CH_2CHMe_2) shown in Figure 2, the $H_{C_1}-H_{C_2}$ distance for primary-B, the shortest contact distance between the olefin methyl and the polymer chain, is 2.07 Å, which was 3.92 Å for primary-A. The $C_\beta-C_\gamma-C_2$ angle between the two groups widens by 13.7° going from primary-A to primary-B to minimize such a steric repulsion. One notices that the $H_{C_3}-H_{indenyl}$ distance, the distance between the polymer chain and the catalyst substituent (2.97 Å), is unchanged between primary-A and primary-B. In Zr**1a**, on the other hand, the $H_{C_3}-H_{CMe}$ distances (2.29 and 2.56 Å), the polymer chain−catalyst distances, and the $H_{C_1}-H_{C_2}$ distance (2.06 Å) become shorter for primary-B in comparison with primary-A. The $C_\beta-C_\gamma-C_2$ angle also widens. Thus one can say that the indirect control energy (6.2 kcal/mol) of Zr**1a** includes the increase in steric energy between the catalyst (the C_{Me} on the indenyl) and the polymer chain (C_3).

The 2-methyl group on the indenyl in Zr**1a** suppresses, as expected, insertion in the secondary-A mode, compared with Zr**1**; the relative energies of the secondary-A for Zr**1a** are larger by 1.8 kcal/mol in the initial stage and 1.3 kcal/mol in the next than the corresponding relative energies for Zr**1**. As seen in the optimized structures for secondary-A mode in Figure 2, the methyl (C_1) of inserting propylene in Zr**1a** is placed in a more congested area than in Zr**1**; the $H_{C_1}-H'_{CMe}$ distance of 2.09 Å in Zr**1a** is shorter than the corresponding $H_{C_1}-H'_{indenyl}$ distance of 2.40 Å in Zr**1**. In the secondary-B mode, the methyl group of inserting propylene is directed to the benzene ring of the indenyl, causing a very large steric energy for both Zr**1** and Zr**1a**.

The 3-methyl on the indenyl in Zr**1b** reduces the energy difference between two primary modes of insertion, since the methyl group of inserting propylene in the primary-A mode has closer contact to the 3-methyl moiety than in the primary-B mode, due to the nonlinear Si−Zr−C_β. As a result, in the initiation stage, the primary-B mode is preferred by 1.1 kcal/mol, while in the propagation stage, the primary-A mode becomes more favorable but only by 2.8 kcal/mol. Thus, stereoregulation by Zr**1b** is expected to be poor.

The substituent effect in 2-methyl-4-alkyl-substituted indenyl catalysts Zr**1c**−Zr**1e** and Zr**1g** has been studied, as also shown in Tables 2 and 3. Compared with the 2-methyl-4-unsubstituted catalyst Zr**1a**, introduction of methyl or ethyl groups at the 4-position in Zr**1c** and Zr**1d** improves the direct control capability a little over 1 kcal/mol, but the indirect controllability is unchanged. When 4-isopropyl is introduced, the catalyst Zr**1e** seems to have substantially better direct and indirect control energies. As shown in Figure 3, the $H_{(isopropyl)}$−propylene H_{C_1} and $H_{Me(isopropyl)}-H_{C_1}$ distances in the primary-B TS, 1.91 and 2.19 Å, respectively, are shorter than the corresponding distances, 1.93 and 2.37 Å, in the primary-A TS and should contribute to the direct control. The methyl group of inserting propylene in the primary-B TS is also placed closer to the polymer chain than in the primary-A with the $C_\alpha-C_\beta-C_1$ angle being 1.4° larger. Even though the $C_\gamma-C_2-C_3$ angle in the primary-B TS opens up by 10.4° compared to that of the primary-A, to release the steric repulsion between the inserting propylene and the last inserted monomer, there is still a difference of 10 kcal/mol in the indirect control energy.

Zr**1f** with only the 4-isopropyl group on the indenyl shows good selectivity between the primary-A and the primary-B: 4.0 (direct control) and 5.1 kcal/mol (indirect control). Compared with Zr**1e** having 2-Me and 4-iso-Pr, the indirect effect decreases by 4.9 kcal/mol, showing that the 2-methyl group makes a significant contribution to the stereoregularity. The lack of 2-Me in Zr**1f** lowers the energy of the secondary-A mode, and thus the stereoregulatory ability of Zr**1f** is expected to be poor. The synergy effect between 2- and 4-substituents is essential to make stereoregular polymerization. The 2-methyl group with the 4-isopropyl provides a large indirect control energy for discriminating primary-A from primary-B and efficiently prevents the secondary

(28) The dominant primary insertion was confirmed by analysis of the polymer end with NMR: (a) Ewen, J. A. *J. Am. Chem. Soc.* **1984**, *106*, 6355. (b) Yang, X. Y.; Stern, C. L.; Marks, T. J. *J. Am. Chem. Soc.* **1995**, *116*, 10015. (c) Leclerc, M.; Brintzinger, H. H. *J. Am. Chem. Soc.* **1995**, *117*, 1651. (d) Gauthier, W. J.; Corrigan, J. F.; Taylor, N. J.; Collins, S. *Macromolecules* **1995**, *28*, 3771. (e) In the present MM calculation, the electronic preference for the dominant primary insertion cannot be identified. In our previous paper with the model catalyst of $Cl_2TiCH_3^+$ we analyzed the origin of regioselectivity in propylene insertion, showing that the electrostatic attraction favors the primary insertion in addition to the larger steric repulsion in the secondary insertion: Kawamura-Kuribayashi, H.; Koga, N.; Morokuma, K. *J. Am. Chem. Soc.* **1992**, *114*, 2359.

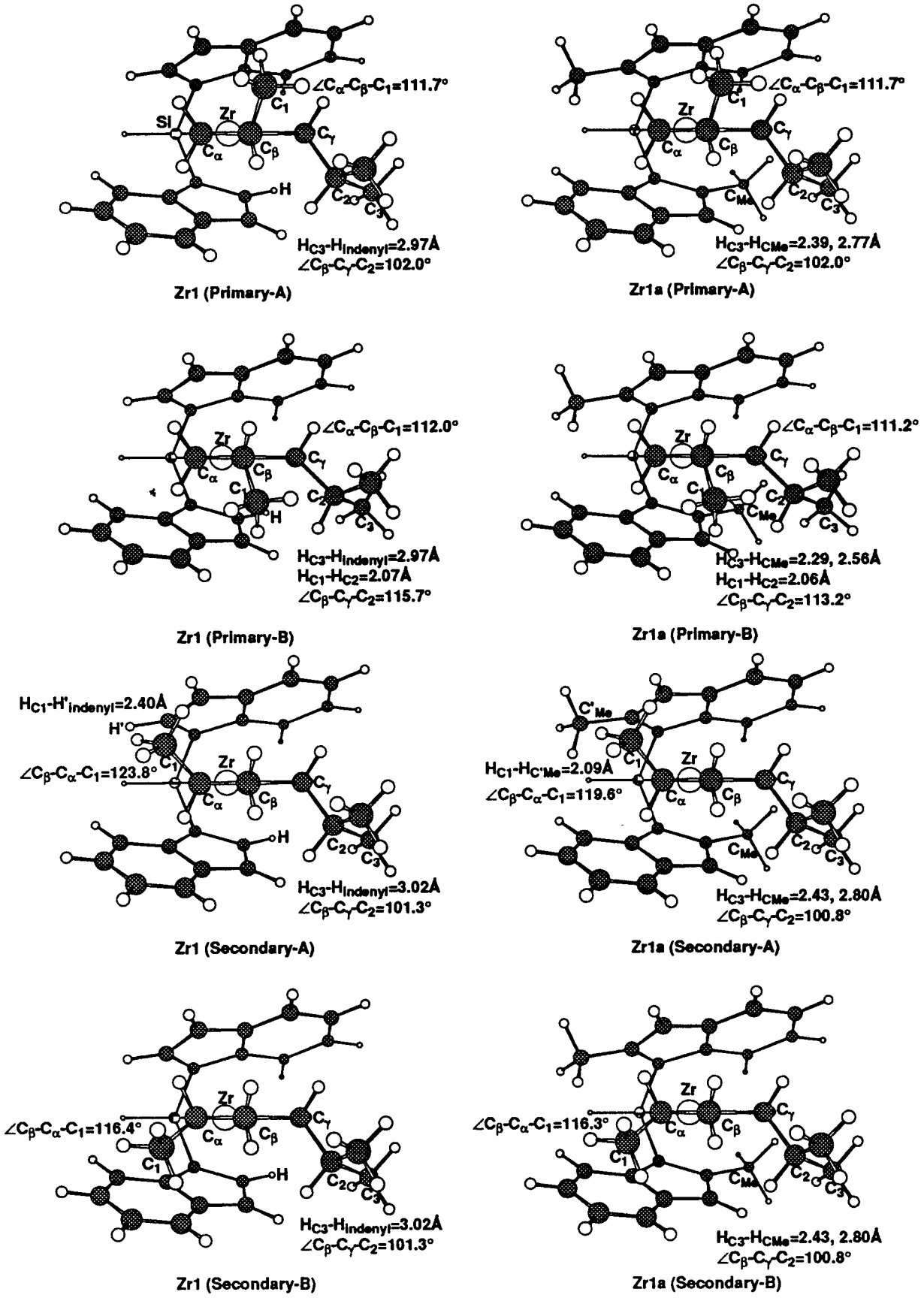

Figure 2. MM-optimized TS structures for primary and secondary propylene insertion to catalysts Zr**1** and Zr**1a** with the polymer chain R = CH_2CHMe_2.

insertion. Note that the indirect control energy difference of 4.9 kcal/mol between Zr**1e** and Zr**1f** includes a contribution from the catalyst−polymer interaction, as mentioned above.

Zr**1g** with the 4-*tert*-butyl group on the indenyl shows the worst capability for isotactic polymerization among 2,4-dialkyl-substituted indenyls Zr**1c**−Zr**1e** and Zr**1g.** Both direct and indirect control energies of Zr**1g** are

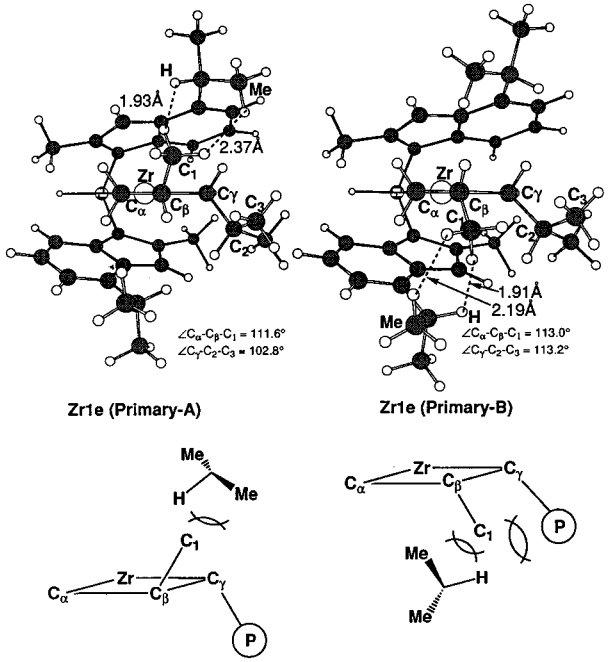

Figure 3. MM-optimized TS structures for primary-A and -B modes of propylene insertion to catalyst Zr**1e** with the polymer chain R = CH_2CHMe_2.

quite small, 2.1 and 1.7 kcal/mol, respectively. It appears that in both primary-A and -B TS's two methyl groups of the *tert*-butyl group are involved in steric repulsion and the reaction site is very congested. Spaleck has confirmed experimentally this inferior selectivity of Zr**1g**.[29] A lesson here is that a tighter reaction site is in general better for energetic discrimination between two primary transition states, but if the reaction site is too congested, both TS's are unstabilized; some flexibility at the transition state seems to be required.

C. Aryl Substitution on the Indenyl Ring, Zr1h−Zr1k. The relative steric energies for catalysts Zr**1h**−Zr**1k** with aryl substituents on the indenyl ring are also shown in Table 3. The direct control energy for Zr**1h** with a 4-phenyl substituent is only 2.0 kcal/mol. However, the indirect control energy is the largest, 14.7 kcal/mol, among the catalysts studied in this paper, and this catalyst should show good stereoregulation capability. As shown in Figure 4, in the propagation stage, two TS's have very different conformations. Compared with the primary-A TS, in the primary-B TS the 4-phenyl group on the indenyl is rotated anticlockwise by the change in the $C_a-C_b-C_c-C_d$ dihedral angle of 49.6° as well as the isopropyl group of the polymer chain around the $C_\gamma-C_2$ bond by the $C_\beta-C_\gamma-C_2-C_3$ dihedral angle change of 70.7°. These rotations are accompanied by a widening of the $C_\beta-C_\gamma-C_2$ bond angle by 21.9° in the primary-B TS. Such large changes can be seen only in Zr**1h** and discriminate energetically the two primary TS's for high stereoregulation.[30]

Compared with 4-phenyl-substituted Zr**1h**, 4-(3-tolyl)-substituted Zr**1i** has a more congested reaction space. However, the energy discrimination is smaller and the

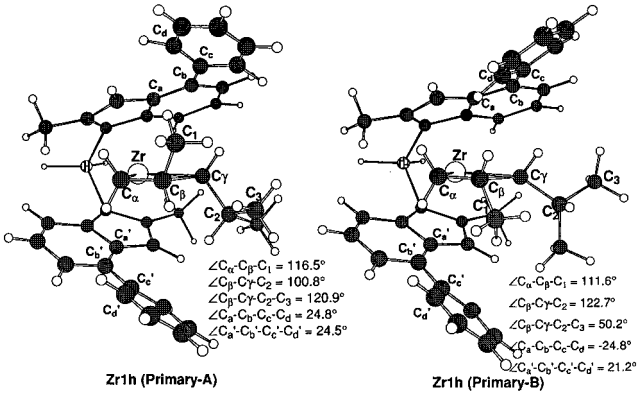

Figure 4. MM-optimized TS structures for primary-A and -B modes of propylene insertion to catalyst Zr**1h** with the polymer chain R = CH_2CHMe_2.

stereoregulation is less effective, with a direct control energy of 1.4 kcal/mol and an indirect control energy of 6.8 kcal/mol. The TS for 4-(1-naphthyl)-substituted Zr**1j** gives slightly better stereoregulation than that for 4-(3-tolyl)-substituted Zr**1i** with direct and indirect control energies of 2.0 and 9.6 kcal/mol, respectively. Among the aryl-substituted catalysts Zr**1h**−Zr**1k**, the 4,5-benz derivative Zr**1k**, with the 4,5-benz moiety far from both the inserted monomer in the primary modes and the propagating polymer, provides the least crowded reaction site and gives the lowest capability for stereoregulation. The stereoregulatory capability of Zr**1k** is similar to those of the 2,4-substituted Zr**1c** and Zr**1d**. Away from the reaction site, the 4,5-benz moiety does not participate in stereoregulatory discrimination, suggesting that a substituent at 5-position of indenyl is not effective. The lack of flexibility in the 4,5-benz moiety may contribute to this.

It is natural to assume that the tighter or more congested the reaction site is, the larger the steric interaction and hence the larger the ability of stereoregulation would be. If the reaction site is not crowded at all, both TS's will be stabilized to the same extent, failing to discriminate one TS from the other. This is in general correct. However, what we learned from the examples of Zr**1h**−Zr**1k** as well as Zr**1g** in the preceding subsection is that tightness is not all and that some flexibility is needed to favor one over the other. If the reaction site is too crowded, both TS's will be destabilized to the same extent, again failing to give a large energy difference between the two TS's. With some flexibility, the more stable primary-A TS can take a substantially different polymer and substituent conformation from the less stable primary-B TS, giving rise to a substantial energy advantage, as shown for Zr**1e** and Zr**1h**.

D. Asymmetric H_2Si(3-*tert*-butylCp)(fluorenyl)ZrMe$^+$ (Zr3a). Finally, our attention is turned to an asymmetric catalyst that can produce the isotactic sequence. As mentioned in Scheme 1, in general, C_s symmetrical catalyst should provide a syndiotactic sequence. However, if either of the two reaction sites in the C_s symmetrical catalyst is completely blocked off by a bulky substituent R′, as shown in Scheme 1C, only one reaction site is active and the isotactic sequence could be regulated.

By introducing a *tert*-butyl substituent at the 3-position, the C_s symmetrical H_2Si(Cp)(fluorenyl)ZrMe$^+$ (Zr**3**)

(29) Spaleck, W. A private communication at Tosoh Corp., 1994.
(30) In the global minimum of Zr**1g** for the primary-B mode, the catalyst loses C_2 symmetry to ease the steric repulsion caused by the polymer chain to the 4-phenyl group and the inserting propylene. Another minimum maintaining C_2 symmetry for the primary-B has higher steric energy than the global minimum by 3.6 kcal/mol.

Table 4. Relative Steric Energies (in kcal/mol) at the Transition States for Propylene Insertion to Catalyst Zr3a[a]

		primary insertion		secondary insertion	
R[b]	insertion site	primary-A	primary-B	secondary-A	secondary-B
Me					
	the hindered site	3.5	0.0	27.1	34.5
	the less-hindered site	−0.6	−3.0	9.0	31.4
$[CH_2CHMe]Me$[c]					
	the hindered site	13.9	0.0	26.1	32.4
	the less-hindered site	22.7	12.2	26.5	48.8

[a] Steric energies are relative to the primary-B for attack from the hindered site. [b] R denotes the polymer chain, as shown in Chart 1.

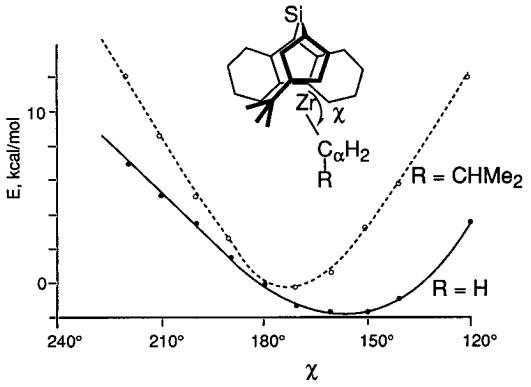

Figure 5. Relative energy of H_2Si(3-tert-butyl Cp)(fluorenyl)$ZrCH_2R^+$ Zr**3a**, as a function of the angle $\chi = \angle Si-Zr-C_\alpha$ with R of $CH_2R = CH_2CHMe_2$ and CH_3.

is converted to an asymmetrical Zr**3a**. For Zr**3a** one can still construct four TS's, i.e., for primary or secondary insertion with the propylene CH_3 above (A) or below (B) the $ZrC_\alpha C_\beta C_\gamma$ plane. First, we have estimated preliminarily whether the hindered vacant site can accept monomer insertion. The dependence of the relative MM steric energy on $\chi = \angle Si-Zr-C$, while freezing all the other geometrical parameters, was examined for Zr**3a**, as shown in Figure 5, where RCH_2 represents the polymer chain. In the initiation stage, where RCH_2 is a methyl group, the energy minimum is found at $\chi = \sim 155°$, as the methyl group can avoid the steric repulsion from the 3-*tert*-butyl group on the Cp ring by bending away from it. After a propylene is inserted (RCH_2 = isopropyl), this polymer chain already has a strong steric contact with the fluorenyl ligand and cannot move away from the 3-*tert*-butyl group. Hence the minimum is confined to the vicinity of 180°, actually found at $\chi = \sim 170°$. From these results, one can say that the monomer must approach the Zr atom from the hindered site, as the polymer chain has already occupied the less-hindered site.

Next, the propylene insertion from both the hindered and the less-hindered sites are examined, as shown in Table 4. Here one notices in general that the primary-B TS has the lowest energy, mainly avoiding the steric repulsion from the 3-*tert*-butyl group. In the initiation stage when the polymer chain is Me, monomer insertion can take place from both the hindered and the less-hindered site. The primary-A mode from the less-hindered site is accessible with 2.4 kcal/mol, and the primary-B from the hindered site with 3.0 kcal/mol above the most favorable primary-B from the less-hindered site, which should lead to the lack of stereoregulatory control in the subsequent insertion. In the propagation stage, represented with R = isopropyl,

Scheme 3. Indirect Control of Stereoregularity with One-Blocked Access: Determination of the Conformation of Polymer Chain End

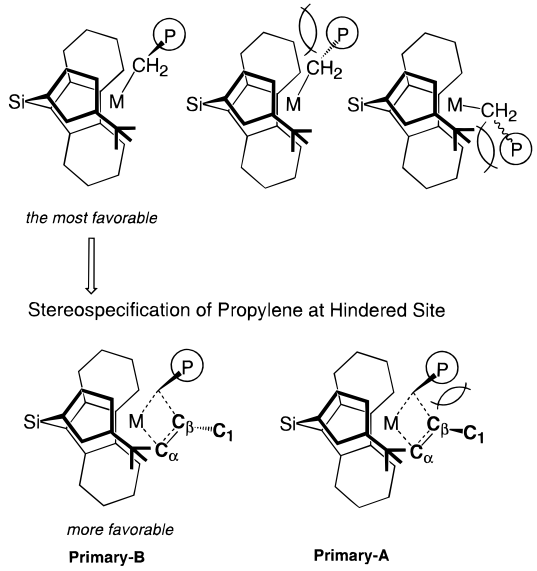

steric repulsion between the 3-*tert*-butyl group and the polymer chain becomes dominant and propylene insertion can take place only in the primary-B mode from the hindered site, providing an isotactic polymer.

Schematic explanation of the stereoregulation mechanism in the propagation step is given in Scheme 3. A comparison of the MM-optimized geometries for the two primary insertion modes at the hindered site is shown in Figure 6. The H−H steric contact between the inserting monomer and the polymer chain in primary-A (at 2.09 Å) is larger than that (at 2.19 Å) in the primary-B. In the primary-A mode, the $C_\beta-C_\gamma-C_2-C_3$ dihedral angle opens up to 140.3° to avoid steric contact between the methyl (C_1) of the inserting monomer and the propagating polymer chain. In the more favorable primary-B mode, the corresponding angle is 69.6°; the methyl group can direct itself to the bay area of the fluorenyl moiety without opening the dihedral angle.

The steric energy difference between the most favorable mode with the next most favorable mode, 12.2 kcal/mol in the propagation state, suggests that the stereoregulating ability of Zr**3a** should be very good, comparable to that of Zr**1e** having 2-methyl-4-isopropylindenyl. Razavi and co-workers found experimentally that Zr**3** having a methyl group at the 3-position of the Cp ring gives a hemiisotactic sequence.[31] It is expected from the above MM result that the methyl substituent, unlike the *tert*-butyl in Zr**3a**, cannot preclude the insertion of monomer from the less-hindered site in the

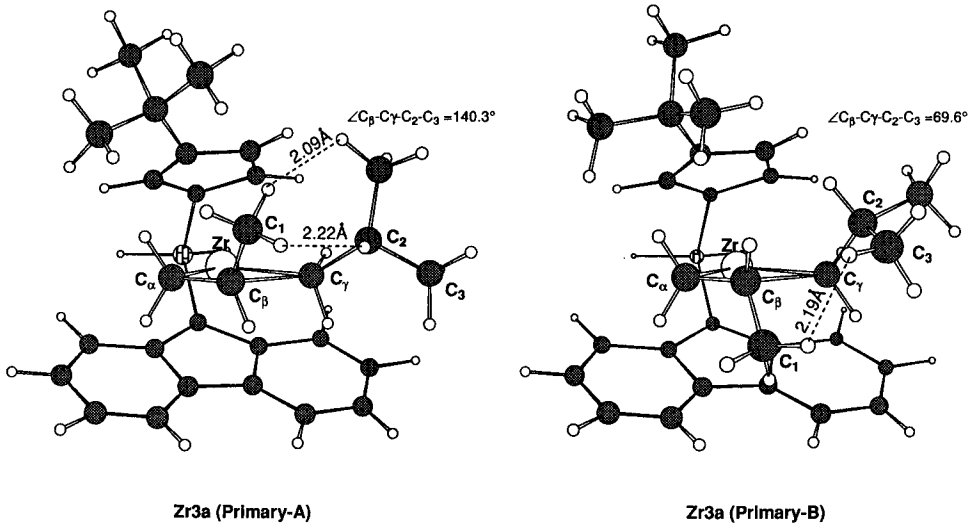

Figure 6. MM-optimized TS structures for primary-A and -B modes of propylene insertion from the hindered site to catalyst Zr**3a** with the polymer chain R = CH_2CHMe_2.

propagation step which would produce mainly *r* diad in alternate sequences.

IV. Relationship between Calculations and Experiments

By using the MM method to evaluate steric energy differences among four different modes of olefin insertion at the ab initio-determined model transition state, we have examined the C_2-symmetric indenyl-based metallocenes for their capability of isotactic control in propylene polymerization. We have divided the steric energy difference into direct control energy (the direct steric energy between the catalyst and the olefin) and indirect control energy (the steric energy between the catalyst and the growing polymer chain on the catalysts and that between the polymer chain and the olefin) and evaluated them separately. For the present series of catalysts, stereoregulation is found to be controlled mainly by the indirect interaction term, as was previously found for related metallocene catalysts.[8,10]

Among group 4 bis(indenyl) and bis(tetrahydroindenyl) complexes, the titanocenes, Ti**1** and Ti**2**, are expected to be intrinsically substantially superior to their zirconium and hafnium analogs in producing an isotactic sequence.[25] The transition states for Ti systems are much tighter than those for Zr and Hf, due to the atomic size of the central metal, and are more sensitive to the steric interaction among substituents, providing better discrimination of one transition state over the others. However, at high reaction temperature, a Ti catalyst having weak bond strength could lose the catalyst structure and thus decrease stereoregulatory capability.[26,27] The zirconocenes, Zr**1** and Zr**2**, and hafnocenes, Hf**1** and Hf**2**, with similar atomic radii for the central metals show similar stereoregulatory capability, being consistent with the experimental results.[2,4b,27]

In Zr**1a** with the 2-methyl group, it was found experimentally by Spaleck et al. that the 2-methyl group of the indenyl improves stereoregulatory ability by inhibiting the secondary insertion.[4c−e] The present MM calculation reveals that indirect control is the predominant factor in stereoregulation, where the 2-methyl group acts as an inhibitor for both indirectly the primary-B and directly the secondary-A modes. It can be also said that the capability of $H_2Si(2,4\text{-}Me_2Cp)_2Zr^+$, previously found to have 0.9 kcal/mol of direct control and 8.5 kcal/mol of indirect control,[10] is better than that of Zr**1a**; this is consistent with the experiment.[4d]

The synergy effect with 2- and 4-substituents is found to be extremely important for stereoregulation, as also experimentally examined.[4c−e] 2-Methyl-4-R-substituted Zr**1e** (R = isopropyl) and Zr**1h** (R = phenyl), with a large indirect control, are the best catalysts among those studied here for formation of an isotactic sequence. The substituent at the 5-position of the indenyl is less effective, as seen in Zr**1k** having 4,5-benz moiety, in agreement with experiment.[4e] Zr**1g** with the 4-*tert*-butyl group, the most congested catalyst, is found to be very poor in stereoregulation, again in agreement with experiment.[29] Compared with Zr**1h** with the 4-phenyl group, such poor performance could also be predicted in the more congested Zr**1i** with the 4-(3-tolyl) group. We have also examined the stereoregulatory capability of the asymmetric catalyst Zr**3a**, where one of the two active sites is blocked by the 3-*tert*-butyl group introduced on the C_s symmetric $H_2Si(Cp)(fluorenyl)ZrR^+$ Zr**3**. In the propagation stage, the steric repulsion between the 3-*tert*-butyl group and the polymer chain becomes dominant and propylene insertion can take place only in the primary-B mode from the hindered site, providing an isotactic polymer with a control capability comparable to Zr**1e** having 2-methyl-4-phenylindenyl. Recently, it was reported that asymmetrical Zr**3a** shows high capability for isotactic regulation.[16b]

From the above discussions, the stereoregulatory capabilities of the Zr catalysts thus examined can be classified as follows: (1) Zr**1b**, Zr**1f**, and Zr**1g** (worst) < (2) Zr**1** and Zr**2** (worse) < (3) Zr**1a** (standard) < (4) $H_2Si(2,4\text{-}Me_2Cp)_2Zr^+$, Zr**1c**, Zr**1d**, Zr**1i**, and Zr**1k** (fair) < (5) Zr**1e**, Zr**1h**, Zr**1j** and Zr**3a** (good). The corresponding experimental results,[4b−e,29,32] where Spaleck

(31) Razavi, A.; Vereecke, D.; Peters, L.; Dauw, K. D.; Nafpliotis, L.; Atwood, J. L. In *Ziegler Catalysts*; Fink, G., Mülhaupt, R., Brintzinger, H. H., Eds.; Springer-Verlag: Berlin, 1995; p 111.

(32) Some additional experimental results of *ansa*-zirconocenes are found in the following references: (a) For Zr**1**, Zr**2**, Zr**1a**, Zr**1e**, Zr**1h**, Zr**1j**, and Zr**1k**, see refs 1c, 4c, 4d, and 4e. (b) For Zr**1b**, see Antberg, M.; Bohm, L.; Luker, H.; Rohrmann, J.; Spaleck, W. EP-399348, 1990. (c) For Zr**1c**, Zr**1d**, and Zr**1i**, see Antberg, M.; Rohrmann, J.; Spaleck,

and co-workers have many contributions, are in line with the present MM calculation results.

To attain high stereoregulation, a catalyst has to possess a certain extent of congested reaction site. However, overcongestion gives too little flexibility for effective discrimination of transition states. A subtle balance between the tightness and the flexibility seems to be essential, and careful theoretical design of the reaction space is indispensable. The combined MO−MM calculation can provide useful information concerning stereocontrol capability and can serve as a predicative tool prior to the experiment.

V. Concluding Remarks

The present combined MO−MM method based on a reasonable TS structure allows evaluation of the controlling factors of stereoregulation and provides results consistent with known experimental results, as discussed in several cases above. Previous computational studies by Corradini[8] and Rappè[9] give similar conclusions to our previous[10] and present studies. However, the use of a π-complex[8] and a "TS-like" π-complex[9] for the stereoregulatory transition state introduces arbitrariness and could lead to some inconsistencies, as discussed in the Introduction.

The present results clearly show that the favorable steric effect at the insertion transition state discriminates one stereospecific transition state from the others. Thus, steric congestion is desirable for a better discrimination. However, what we have found is that overcongestion is detrimental to the steric selection. Apparently the loss of flexibility makes all the transition states uniformly less favorable and the discrimination more difficult. A subtle balance between these has to be found for the best result.

In the experimental design of the catalyst, the rigidity is considered to be an important factor for maintaining the stereoregulatory ability and high reactivity during the polymerization reaction. For these purposes, catalysts having the rigid bridged structures, such as diphenyl methylene bridge[33a] or diphenyl silylene bridge,[33b] have been reported. An extension of the present approach to these systems would provide theoretical prediction and insight into the factors determining stereoregulatory ability.

In the present paper, we at first optimized the transition state for ethylene insertion to the unsubstituted catalysts having a short (R = Me) growing polymer chain on the metal, **4**TS and Zr**3**TS, and, upon freezing the geometry of these active parts of the transition state (except for the position of the hydrogen atoms replaced), we optimized with the MM method the geometries of substituents on the catalyst, the methyl group on propylene and the alkyl group of growing polymer chain. In reality, the structure of the transition state is expected to change by these substituents, especially when the steric energy among the substituents is large. One should, if possible, fully optimize all the transition states for different substituents and different approaches. The full ab initio determination of such transition states for catalysts with large substituents is expensive and impractical. We have recently developed a new "integrated molecular orbital + molecular mechanics" (IMOMM) method,[34] in which the total energy (and its gradient and second derivatives as well) of a large "real" system is defined as a sum of the ab initio molecular orbital energy of the small "model" system and the molecular mechanics energy of the "real" system excluding the ab initio contribution. The geometry of transition states as well as equilibrium structures can be optimized fully for this integrated MO + MM energy. The IMOMM method is ideally suited for study of the changes of transition states and their energetics with multiple substituents. Application of the IMOMM method to studies of the rate and the regio- and stereoselectivity of olefin polymerization by metallocene catalysts is in progress in our laboratories and will be reported in the future.

Acknowledgment. All numerical calculations were carried out at the Institute for Molecular Science and at Cherry L. Emerson Center for Scientific Computation at Emory University. T.Y. was a visiting research fellow at IMS and Nagoya University. T.Y. is grateful to A. Yano, M. Sone, and the members of Polymer Synthesis Division at Tosoh for helpful discussions about the experimental results. This research was supported in part by grants-in-aid from the Ministry of Education, Science and Culture of Japan and by a grant from the U.S. National Science Foundation.

OM9504009

W. EP-530647, 1993. (d) For Zr**1g**, see ref 29. (e) For Zr**3a**, see ref 16.

(33) (a) Razavi, A; Atwood, J. L. *J. Organometal. Chem.* **1993**, *459*, 117. (b) Spaleck, W.; Antberg, M.; Dolle, V.; Klein, R. Rohrmann, J.; Winter, A. *New J. Chem.* **1990**, *14*, 499.

(34) (a) Maseras, F.; Morokuma, K. *J. Comput. Chem.* **1995**, *16*, 1170. (b) Matsubara, T.; Maseras, F.; Koga, N.; Morokuma, K. *J. Phys. Chem.*, in press.